Title

Temperature-dependent growth of hexagonal and monoclinic gallium sulfide films by pulsed-laser deposition

Permalink

https://escholarship.org/uc/item/4002z357

Journal

AIP Advances, 10(10)

ISSN

2158-3226

Authors

Eriguchi, Kazutaka
Biaou, Carlos
Das, Sujit
et al.

Publication Date

2020-10-01

DOI

10.1063/5.0021938

Peer reviewed

Temperature-dependent growth of hexagonal and monoclinic gallium sulfide films by pulsed-laser deposition

Cite as: AIP Advances **10**, 105215 (2020); https://doi.org/10.1063/5.0021938
Submitted: 15 July 2020 . Accepted: 23 September 2020 . Published Online: 08 October 2020

Kazutaka Eriguchi, Carlos Biaou, Sujit Das, Kin Man Yu, Junqiao Wu, and Oscar D. Dubon

AIP Advances **10**, 105215 (2020); https://doi.org/10.1063/5.0021938

Temperature-dependent growth of hexagonal and monoclinic gallium sulfide films by pulsed-laser deposition

Cite as: AIP Advances 10, 105215 (2020); doi: 10.1063/5.0021938
Submitted: 15 July 2020 • Accepted: 23 September 2020 •
Published Online: 8 October 2020

Kazutaka Eriguchi,[1,2,3,a)] **Carlos Biaou,**[4] **Sujit Das,**[1] **Kin Man Yu,**[5] **Junqiao Wu,**[1,2] **and Oscar D. Dubon**[1,2,b)]

AFFILIATIONS

[1] Department of Materials Science and Engineering, University of California, Berkeley, California 94720-1760, USA
[2] Materials Sciences Division, Lawrence Berkeley National Laboratory, Berkeley, California 94720, USA
[3] Advanced Evaluation and Technology Development Department Technology Division, Sumco Corporation, 1-52 Kubara, Yamashiro-cho, Imari-shi, Saga 849-4256, Japan
[4] Applied Science and Technology, University of California, Berkeley, California 94720-1760, USA
[5] Department of Physics, City University of Hong Kong, 83 Tat Chee Ave., Kowloon, Hong Kong SAR, China

[a)] kazerigu@sumcosi.com
[b)] **Author to whom correspondence should be addressed:** oddubon@berkeley.edu

ABSTRACT

We demonstrate the selective, pulsed-laser deposition of hexagonal GaS and monoclinic Ga_2S_3 films on sapphire substrates from a single Ga_2S_3 target in high-vacuum conditions. Growth at substrate temperatures below 550 °C causes GaS film formation, which indicates non-stoichiometric transfer from the target to the film. Surprisingly, stoichiometric transfer occurs at substrate temperatures above 650 °C with monoclinic Ga_2S_3 as the preferred, higher S-content phase. Through a series of growth and annealing experiments, we show that GaS nucleation under S-deficient conditions leads to the preferred growth of this layered, hexagonal phase below 550 °C. Furthermore, GaS films annealed above 650 °C under high vacuum are transformed to Ga_2S_3, reflecting the greater stability of the monoclinic phase. By first growing Ga_2S_3 at a higher temperature and subsequently growing GaS at a lower temperature, we can fabricate GaS/Ga_2S_3 heterostructures in a single growth process.

I. INTRODUCTION

Gallium sulfide is a group III–VI semiconductor with multiple stable phases, including the (layered) hexagonal GaS phase and monoclinic Ga_2S_3 phase. GaS has been employed in a variety of applications that require ultrathin layers, including transistors and photodetectors, and is an attractive candidate for flexible electronics.[1–3] The layered GaS structure is composed of Ga–Ga and Ga–S covalent bonds that extend in two dimensions while interlayer bonding occurs via van der Waals interaction. At room temperature, the bandgap of GaS is ~2.6 eV.[4,5] Another form of gallium sulfide, the monoclinic Ga_2S_3 phase, consists of covalent bonds in three dimensions (i.e., not layered) and has a reported bandgap of ~3.0 eV.[6–8]

Thin GaS and Ga_2S_3 films have been grown using a variety of methods, including chemical vapor deposition (CVD), chemical vapor transport (CVT), and chemical bath deposition (CBD).[9–15] Studies using these methods have demonstrated that depending on growth conditions, GaS, Ga_2S_3, or a combination of both phases is synthesized. More recently, one report of gallium sulfide growth was achieved by physical vapor transport (PVT) using GaS powder as the source material. GaS was found to grow at 670 °C while Ga_2S_3 formed at 800 °C. Between these two temperatures, both phases co-existed in the film. This growth behavior was attributed to the temperature-dependent, vapor pressure difference between gallium and sulfur species.[16] Other materials systems exhibiting similar III–VI and III_2–VI_3 growth behaviors are gallium selenide[17] and indium selenide.[18]

Here, we demonstrate the selective pulsed-laser deposition (PLD) of hexagonal GaS and monoclinic Ga_2S_3 films on sapphire substrates from a single Ga_2S_3 target in high-vacuum conditions. Until now, PLD has been considerably less explored but possesses characteristics that are attractive for layered material synthesis. Specifically, PLD is a physical vapor process that enables "digital" deposition of target materials using a pulsed laser to supply energy for source material evaporation.[19–22] For example, PLD has been used to grow few-layer nanosheets of layered GaSe.[23]

II. EXPERIMENTAL

Gallium sulfide films were deposited onto c-Al_2O_3 (0001) (sapphire) substrates using the PLD technique (with a KrF excimer laser with a wavelength of 248 nm and pulse duration of 20 ns). Before deposition, each substrate underwent ultrasonic cleaning in isopropyl alcohol and oxygen plasma cleaning. Epitaxial films were obtained from a single Ga_2S_3 target. Compared to GaS, Ga_2S_3 has a higher sulfur content, which may be helpful in addressing possible sulfur deficiency in films; chalcogen deficiency can present a challenge in PLD. The base pressure in the PLD chamber was maintained at less than 3×10^{-6} Torr. The distance between the target and the substrate was fixed at 7 cm. The laser energy density was set to 1.6 J/cm^2, and the pulse repetition rate was 1 Hz. The substrate temperature ranged from 22 °C to 700 °C. The deposition time was set to one hour. Samples were then characterized using Rutherford backscattering spectrometry (RBS) with 3.04 MeV $^4He^{2+}$ to evaluate the chemical composition ratio and film thickness. RBS data were analyzed using the SIMNRA software package (https://home.mpcdf.mpg.de/~mam/). Raman spectroscopy using a 488 nm excitation laser and X-ray diffraction (XRD) using Cu Kα radiation provided the structural analysis. The domain size was obtained by analyzing the (002) and (111) diffraction peaks of GaS and Ga_2S_3, respectively, using the Scherrer equation.[24]

III. RESULTS AND DISCUSSION

Figure 1 shows the RBS spectra of films deposited at a substrate temperature from 500 °C to 700 °C. The chemical composition and thickness of the films are presented in Table I. Below 550 °C, the Ga-to-S ratio is 1:1; from 550 °C to 650 °C, the relative amount of Ga gradually decreases (i.e., the films contain more S than Ga); and above 650 °C, the Ga-to-S ratio reaches a stable value of 2:3. In addition, the narrowing of the S and Ga signals in the RBS spectra as the substrate temperature increases shows that the films become correspondingly thinner (by over a factor of 2) despite otherwise similar growth conditions (i.e., deposition time, laser fluence, and pulse rate). This is not surprising as the sticking coefficient of vapor species impinging on the surface should decrease with increasing temperature—a commonly observed trend in physical vapor deposition, particularly for high vapor-pressure species. We note that GaS films as thin as 9.4 nm have been grown (see the supplementary material, Figs. S1 and S2).

Figure 2 shows the Raman spectra for films deposited at each growth temperature. For growth temperatures in the range of 500 °C–575 °C, the peaks that originated from GaS ($A^1{}_{1g}$, $E^1{}_{2g}$, and $A^2{}_{1g}$) are observed.[22] At 600 °C, peaks associated with Ga_2S_3 appear at 235 cm^{-1} and 146 cm^{-1} (not shown).[25,26] The co-existence of peaks associated with both GaS and Ga_2S_3 indicates the presence of both gallium sulfide phases. In the temperature range in which GaS and Ga_2S_3 Raman peaks co-exist, a nominal Ga:S composition ratio between 1:1 and 2:3 is expected. We observed such a change in composition in the RBS spectra in Fig. 1 and report it in Table I. Above 650 °C, the peaks that originate from GaS are absent, and only peaks originating from Ga_2S_3 are observed.

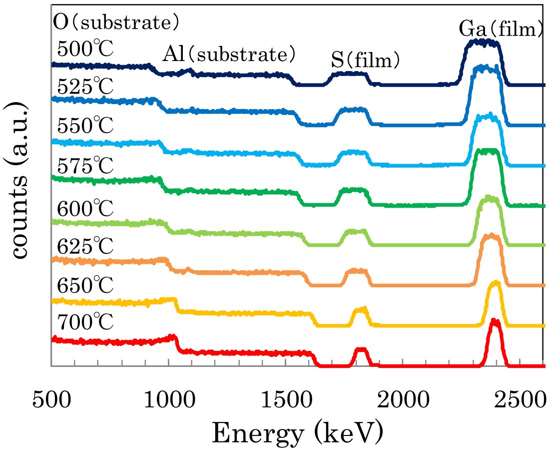

FIG. 1. Rutherford backscattering spectra of the samples at each growth temperature. Film thicknesses range from 199 nm at 500 °C to 80 nm at 700 °C.

TABLE I. Chemical composition and thickness at various growth temperatures determined from RBS spectra presented in atomic percent (at. %).

Growth temperature (°C)	Ga (at. %)	S (at. %)	Thickness (nm)
500	49.5	50.5	199
525	49.8	50.2	170
550	49.8	50.2	158
575	48.0	52.0	156
600	46.0	54.0	136
625	45.8	54.2	123
650	40.5	59.5	83
700	40.0	60.0	80

Figure 3 shows the XRD patterns of the films deposited for each sample at growth temperatures of 525 °C, 600 °C, and 650 °C. All samples display a sharp peak at 20.5° from the (0003) plane of the sapphire single-crystal substrate.[27] GaS (002) and (004) diffraction peaks were observed at 525 °C.[28] The (111) diffraction peak of Ga_2S_3 emerged at 600 °C. At 650 °C, the GaS diffraction peaks are not present, and only peaks associated with Ga_2S_3 and the sapphire substrate remain.[12] These structural results are consistent with both Raman spectroscopy and RBS measurements and confirm the existence of three regions: at the low-temperature range (500 °C–550 °C), GaS forms; at intermediate temperatures, both GaS and Ga_2S_3 grow; and at the high-temperature range (≥650 °C),

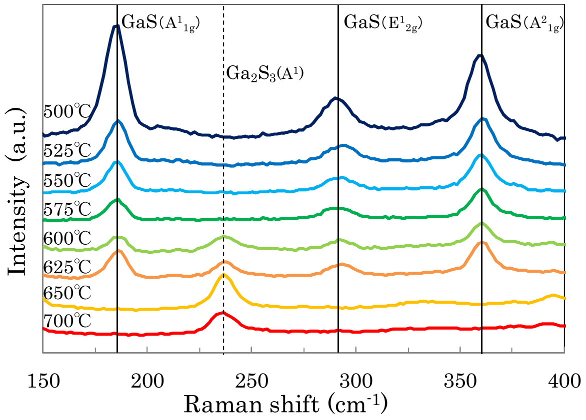

FIG. 2. Raman spectra of synthesized films at different growth temperatures—from top to bottom, 500 °C, 525 °C, 550 °C, 575 °C, 600 °C, 625 °C, 650 °C, and 700 °C. The spectra of the films transition from showing peaks from only GaS at low temperature, to peaks from a mixture of GaS and Ga_2S_3 at intermediate temperatures, to peaks from only Ga_2S_3 at elevated temperatures.

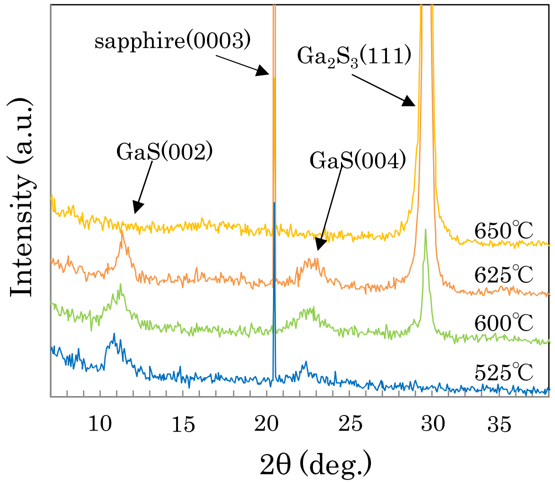

FIG. 3. X-ray diffraction patterns for films deposited on sapphire at different deposition temperatures. The film deposited at 650 °C is single-phase, monoclinic Ga_2S_3. At 625 °C and 600 °C, the films consist of a phase mixture, monoclinic Ga_2S_3 and hexagonal GaS. The film deposited at 525 °C shows peaks associated with GaS.

Ga_2S_3 forms exclusively. The diffraction peaks are broader for the GaS than the Ga_2S_3 phases, indicating that the films are defective and polycrystalline with small domain sizes (<10 nm for GaS and <30 nm for Ga_2S_3) (see the supplementary material, Table S1). Nonetheless, the films are strongly textured; notably, only the (002) and (004) diffraction peaks are present for the GaS films, indicating *c*-axis (out of the plane) preferred orientation.

To understand why GaS films grow from a Ga_2S_3 target at lower temperatures, we have performed a combination of growth and annealing experiments. Table II presents the sample structures and annealing temperatures. Figure 4 shows the Raman spectrum for each sample after experiments. First, we deposited a Ga_2S_3 film, or buffer layer, at 650 °C, subsequently cooled the sample to 525 °C, and deposited a second film at that temperature. This resulted in a bilayer structure of GaS on Ga_2S_3 (on sapphire) (sample A). The GaS film is strongly *c*-axis textured (see the supplementary material, Figs. S3 and S4) displaying not only the (002) and (004) peaks of GaS but also the (006) peak. We prepared another sample by growing a Ga_2S_3 buffer layer on sapphire and cooling it to room temperature; then, we deposited another film on top of the buffer layer (sample B). In this case, the film deposited at room temperature was amorphous. Subsequently, we annealed the sample in the PLD growth chamber at 525 °C for one hour. The Raman spectrum for this sample shows evidence of only Ga_2S_3, indicating that the amorphous film transforms to Ga_2S_3 by solid-phase epitaxy (SPE). This behavior is consistent with the theory of intrinsic SPE, whereby the buffer layer seeds solid-phase homoepitaxy with no barrier to nucleation.[29]

In the absence of a Ga_2S_3 buffer layer, an amorphous film deposited directly on sapphire and annealed at 525 °C crystallizes predominantly in the layered GaS phase (sample C); the Raman spectrum contains a strong peak from GaS and a small signal that may be attributed to the Ga_2S_3 phase. This suggests that the enhancement of S locally in the solid phase (amorphous film) enables nucleation of some Ga_2S_3 even as most of the film crystallizes as GaS. We note that the amorphous films have a Ga:S atomic composition near 1:1 despite the use of a Ga_2S_3 target.

A fourth sample (D) was prepared by first depositing a GaS film on sapphire at 525 °C followed by an amorphous film at room temperature. The sample was then annealed at 650 °C. Following annealing, the Raman spectrum shows evidence of only Ga_2S_3, demonstrating that this is the more stable phase at elevated temperature under high-vacuum conditions—specifically, the GaS buffer layer underwent a sold-phase transformation to Ga_2S_3.

The successful SPE of Ga_2S_3 from a Ga_2S_3 buffer layer suggests that conditions could exist that will lower the temperature for Ga_2S_3 nucleation and growth; that is, experimental parameters in PLD may exist to drive a preference for the formation of Ga_2S_3 over

TABLE II. Pulse-laser-deposited films and annealing temperature.

Sample	Synthesized film structure	Annealing temperature	Film phase(s) after annealing
A	GaS(epi)/Ga_2S_3(epi)/sapphire	N/A	N/A
B	Amorphous Ga–S/Ga_2S_3(epi)/sapphire	525 °C	Ga_2S_3
C	Amorphous Ga–S/sapphire	525 °C	GaS (major) Ga_2S_3 (minor)
D	Amorphous Ga–S/GaS(epi)/sapphire	650 °C	Ga_2S_3

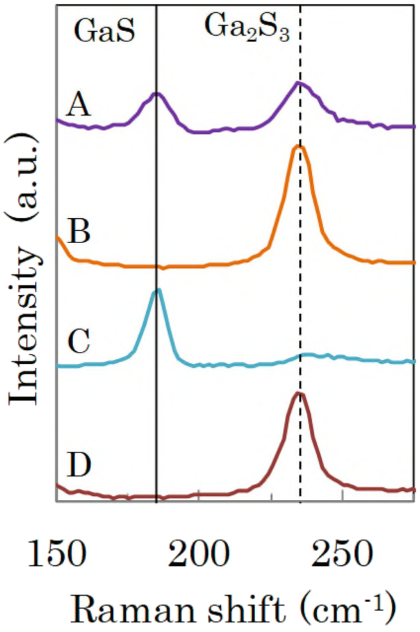

FIG. 4. Raman peaks of films deposited on sapphire substrates and subsequently annealed in the PLD chamber. They are from top to bottom: GaS(epi)/Ga_2S_3(epi)/sapphire as-grown (A); amorphous Ga-S/Ga_2S_3(epi)/sapphire annealed at 525 °C (B); amorphous Ga-S/sapphire annealed at 525 °C (C); and amorphous Ga-S/GaS(epi)/sapphire annealed at 650 °C (D).

GaS at lower temperatures. In physical vapor deposition processes, this might be accomplished by either modifying deposition fluxes or changing the substrate. To test this hypothesis, we substituted sapphire substrates with Si substrates in three different orientations—Si (111), Si (110), and Si (100)—and deposited films under the PLD conditions described previously. The measured Raman spectra are presented in Fig. S5 and used to identify the phase(s) present in the film as done previously. Table S2 summarizes our findings, which show that indeed, Ga_2S_3 can grow at lower temperatures on Si than sapphire. Therefore, we see that both substrate material and crystal orientation provide control over phase nucleation across temperature.

The standard Gibbs free energy of formation of Ga_2S_3 is lower than GaS over the growth-temperature range (500 °C–700 °C).[30] However, under our growth conditions—namely, high vacuum—GaS is the preferred thin-film phase at low temperature. Growth under S-deficient conditions favors the nucleation of GaS over Ga_2S_3. At higher temperatures, Ga_2S_3 nucleation is preferred even under S-deficient conditions, and GaS no longer grows. The nucleation behavior can be controlled by the substrate material and orientation, pushing Ga_2S_3 growth to lower temperature. The amorphous and GaS films transform to Ga_2S_3 upon annealing at 650 °C, demonstrating the greater stability of Ga_2S_3 at higher temperature under the experimental conditions used; using a sapphire substrate, we were not able to grow a Ga_2S_3 at 650 °C on a previously grown GaS film as the GaS film undergoes a solid-phase transformation to Ga_2S_3 at this temperature.

IV. CONCLUSION

In summary, pulsed-laser deposition under high vacuum conditions can be used to grow GaS and Ga_2S_3 films from a single Ga_2S_3 target. While stoichiometric transfer occurs at temperatures above 650 °C, the lower-sulfur-content GaS phase is preferred below 550 °C. By changing the substrate temperature within a narrow range, heterostructures of hexagonal (layered) GaS and monoclinic (non-layered) Ga_2S_3 can be synthesized from a single process, providing unprecedented opportunities to realize heterojunctions from a single materials system and investigate the heteroepitaxy of van der Waals semiconductors on three-dimensional, covalently bonded semiconductors.

SUPPLEMENTARY MATERIAL

See the supplementary material for the RBS and Raman spectra of a sub-10-nm-thick GaS film are presented. In addition, the calculated crystalline domain sizes of GaS and Ga_2S_3—obtained from analysis of XRD peaks—are presented. Finally, the Raman spectra and phase information of gallium sulfide films grown on silicon substrates are reported.

ACKNOWLEDGMENTS

This work was supported by the Electronic Materials Program, funded by the Director, Office of Science, Office of Basic Energy Sciences, Materials Sciences and Engineering Division of the US Department of Energy under Contract No. DE-AC02-05Ch11231. O.D.D. recognizes that this work was performed at the Berkeley Lab and UC Berkeley, which sit on the territory of Huichin, the ancestral and unceded land of the Chochenyo speaking Ohlone people, and that every member of the Berkeley community continues to benefit from the use and occupation of this land. Publication made possible in part by support from the Berkeley Research Impact Initiative (BRII) sponsored by the UC Berkeley Library.

DATA AVAILABILITY

The data that support the findings of this study are available within the article and its supplementary material.

REFERENCES

[1] D. J. Late, B. Liu, J. Luo, A. Yan, H. S. S. R. Matte, M. Grayson, C. N. R. Rao, and V. P. Dravid, Adv. Mater. **24**, 3549 (2012).
[2] P. Hu, L. Wang, M. Yoon, J. Zhang, X. Wang, Z. Wen, J. C. Idrobo, Y. Miyamoto, D. B. Geohegan, and K. Xiao, Nano Lett. **13**, 1649 (2013).
[3] S. Yang, Y. Li, X. Wang, N. Huo, J.-B. Xia, S.-S. Li, and J. Li, Nanoscale **6**, 2582 (2014).
[4] T. Aono, K. Kase, and A. Kinoshita, J. Appl. Phys. **74**, 2818 (1993).
[5] C. H. Ho and S. L. Lin, J. Appl. Phys. **100**, 083508 (2006).
[6] C. Ho and H. Chen, Sci. Rep. **4**, 6143 (2014).
[7] H. F. Liu, K. K. Ansah Antwi, C. S. Chua, J. Huang, S. J. Chua, and D. Z. Chi, ECS Solid State Lett. **3**(11), 131 (2014).
[8] M. Isk, N. M. Gasanly, and L. Gasanova, Opt. Mater. **86**, 95 (2018).
[9] A. N. MacInnes, M. B. Power, and A. R. Barron, Chem. Mater. **4**, 11 (1992).
[10] A. N. MacInnes, M. B. Power, and A. R. Barron, Chem. Mater. **5**, 1344 (1993).
[11] A. R. Barron, Adv. Mater. Opt. Electr. **5**, 245 (1995).
[12] S. Suh and D. M. Hoffman, Chem. Mater. **12**, 2794 (2000).

[13] A. Harvey, C. Backes, Z. Gholamvand, D. Hanlon, D. McAteer, H. C. Nerl, E. McGuire, A. Seral-Ascaso, Q. M. Ramasse, N. McEvoy, S. Winters, N. C. Berner, D. McCloskey, J. F. Donegan, G. S. Duesberg, V. Nicolosi, and J. N. Coleman, Chem. Mater. **27**, 3483 (2015).

[14] X. Wang, Y. Sheng, R.-J. Chang, J. K. Lee, Y. Zhou, S. Li, T. Chen, H. Huang, B. F. Porter, H. Bhaskaran, and J. H. Warner, ACS Omega **3**, 7897 (2018).

[15] H. Ertap, T. Baydar, M. Yüksek, and M. Karabulut, Turk. J. Phys. **40**, 297 (2016).

[16] J. Kim, W. Park, J.-H. Lee, and M.-J. Seong, Nanotechnology **30**, 384001 (2019).

[17] S.-H. Lee, Y.-K. Hsu, H.-C. Hsu, C.-S. Chang, and W.-F. Hsieh, Jpn. J. Appl. Phys., Part 1 **42**, 5217 (2003).

[18] N. Balakrishnan, E. D. Steer, E. F. Smith, Z. R. Kudrynskyi, Z. D. Kovalyuk, L. Eaves, A. Patanè, and P. H. Beton, 2D Mater. **5**, 035026 (2018).

[19] M. S. Donley, P. T. Murray, S. A. Barber, and T. W. Haas, Surf. Coat. Technol. **36**, 329 (1988).

[20] T. A. J. Loh, D. H. C. Chua, and A. T. S. Wee, Sci. Rep. **5**, 18116 (2015).

[21] Z. Yang and J. Hao, J. Mater. Chem. C **4**, 8859 (2016).

[22] M. J. Taylor, J. Raman Spectr. **1**, 355 (1973).

[23] M. Mahjouri-Samani, R. Gresback, M. Tian, K. Wang, A. A. Puretzky, C. M. Rouleau, G. Eres, I. N. Ivanov, K. Xiao, M. A. McGuire, G. Duscher, and D. B. Geohegan, Adv. Funct. Mater. **24**, 6365 (2014).

[24] P. Scherrer, Göttinger Nachr. Math. Phys. **2**, 98 (1918).

[25] C. Jastrzebski, K. Olkowska, D. J. Jastrzebski, M. Wierzbicki, W. Gebicki, and S. Podsiadlo, J. Phys.:Condens. Matter. **31**, 075303 (2019).

[26] C.-H. Ho, M.-H. Lin, Y.-P. Wang, and Y.-S. Huang, Sens. Actuators, A **245**, 119 (2016).

[27] S. Nakagomi and Y. Kokubun, J. Cryst. Growth **349**, 12 (2012).

[28] X. A. Cao, H. T. Hu, Y. Dong, and X. Y. Hou, J. Appl. Phys. **86**(12), 6940 (1999).

[29] B. C. Johnson, J. C. McCallum, and M. J. Aziz, "Solid-phase epitaxy," in *Handbook of Crystal Growth*, Part A. Thin Films and Epitaxy: Basic Techniques Vol. III, 2nd ed., edited by T. F. Kuech (Elsevier/North Holland, Boston, 2015), pp. 317–363.

[30] V. P. Vasil'ev, Inorg. Mater. **43**(2), 115 (2007).